DOI: 10.21062/mft.2025.015 http://www.journalmt.com

Comparison of Optical Scanners for Reverse Engineering Applications on Glossy Freeform Artifact Pharaoh

Michal Koptis (0000-0001-6598-7895), Jiri Resl (0009-0007-3800-9093), Jan Urban (0000-0002-7208-0981), Jan Simota (0000-0001-7634-182X), Jiri Kyncl (0000-0002-2161-3004), Petr Mikes (0000-0003-3041-4629), Libor Beranek (0000-0003-3190-2405)
Faculty of Mechanical Engineering, Czech Technical University in Prague. Technická 1902/4, 160 00 Praha 6. Czech Republic. E-mail: michal.koptis@fs.cvut.cz

Article deals with analysis on influence of post-process settings profiles in the Polyworks software and its influence on measuring bias (difference between average surface profile deviation and artifacts reference value) and standard deviation of measured data. The comparison was evaluated on glossy artifact with freeform surfaces. Setting with least bias and standard deviation was than used to evaluate repeatability and systematic measurement error and minimum tolerance bandwidth Tmin according to VDA 5 and MSA 4, respectively for three conceptions of laser scanning technologies available on today's market. Cartesian CMM LK Altera S with laser scanner Nikon LC15Dx (automated technology), Measuring arm Nikon MCAx S30 with laser scanner Nikon H120 (manual technology) and optically tracked handheld device Metronor M-Scan with laser scanner Nikon H120 (manual technology). The conclusions of the study can serve as a guide in technology selection for reverse engineering input data acquisition. Subsequently, the optimal parameters of the post-process settings (for glossy surfaces) in the Polyworks software are listed.

Keywords: Freeform reverse engineering, 3D laser scanners accuracy, Glossy artifact, Measurement capability

1 Introduction to the reverse engineering technology

In the modern industrial environment, where competition is constantly increasing and requirements for quality and precision are increasingly strict, the accuracy of measuring devices plays a key role in the field of reverse engineering technology. Reverse engineering has become an essential tool for the analysis and reproduction of complex geometrical shapes, especially in case of freeform surfaces. The technology is widely used in industries such as automotive, aerospace, energy and precision engineering. Measurement accuracy relates to success of entire reverse engineering process. As the capabilities and applications of measurement technologies expand, it is essential to understand the various aspects that affect measurement results, including the calibration of equipment, selection of appropriate measurement methods and minimization of errors caused by external factors. For example, incorrectly selected parameters during measurement or data processing could lead to wrong results. Scanning of "hard-to-scan" surfaces is a challenge for reverse engineering. This article describes the behaviour of scanning systems on a real high-gloss artifact. The output will be a comparison of measuring systems from a point of view of capability coefficients used in the automotive industry. The aim of this article is to provide an overview of current measurement systems used in industrial reverse engineering with a particular focus on data collection from glossy freeform surfaces. The main objective is to perform a comparison of the three scanning systems on the gloss freeform artifact.

2 State of the art

Reverse engineering is an important technology in modern industrial applications that involves the process of analyzing parts or re-designing a product to replicate or improve an original object. The competitive nature of the industrial environment requires constant innovation and improvement. Reverse engineering serves as a bridge between existing products and innovative solutions allowing manufacturers to disassemble and understand a competitive product, outdated systems or parts without original documentation. The essence of this technology lies in its ability to deconstruct an object and create a digital twin that can be evaluated, edited and improved. Reverse engineering is not a monolithic process, but a set of different methods adapted to the object under investigation. [1], [2]

2.1 Reverse engineering methodology

Process typically begins with data acquisition where physical dimensions are captured using 3D scanners or coordinate measuring machines. This is

followed by data processing where the collected data is converted into a digital 3D model (digital twin). The final stages involve analysing the model to understand its function and designing a new part or system that replicates or improves upon the original. [1], [2], [3]. Chronological process of reverse engineering is shown in Figure 1.

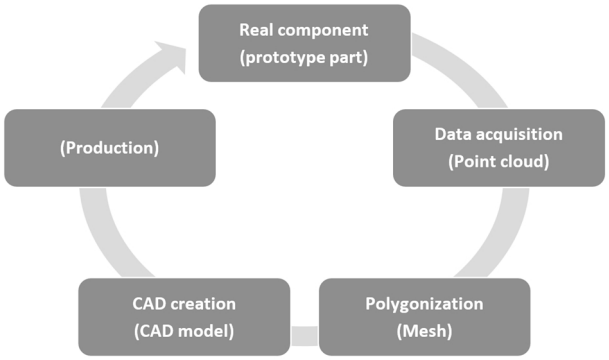

Fig. 1 *Reverse engineering methodology [1]*

The advancement of measuring technologies has greatly enhanced the reverse engineering process. 3D laser scanners and CMMs offer high-precision measurements of complex geometries. Software solutions for Computer-Aided Design (CAD) are crucial for creating accurate representations of scanned data. Additionally, technologies such as 3D printing facilitate rapid prototyping of redesigned components.[1]

2.2 Reverse engineering application

In the field of industrial production of freeform surfaces, when a CAD model is not available, reverse engineering enables the shortening of the product development cycle and the reduction of production costs. The study [4] shows that the correct density of point clouds in high curvature zones is essential to achieve an accurate CAD model. In the shipping industry, this technology facilitates the creation of 3D CAD models of components based on digitization data, ensuring high CAD model accuracy [5]. A significant innovation in the field of reverse engineering is the calibration of the integrated measuring system, which, thanks to the use of a laser scanner, enables the measurement of complex shapes with high accuracy, even when measuring thin or self-enclosed surfaces [6]. The use of digital twins in robotic measurement of freeform surfaces is another step to increase the efficiency and autonomy of measurement processes, thanks to advanced features such as sensor simulations and path planning [7]. Reverse engineering makes it possible to obtain component geometries that are otherwise unavailable. An example is the digitization of mechanical components using 3D scanning, where a 3D image of a broken impeller was created [8]. When prototyping using additive manufacturing, reverse engineering proves to be an effective method where the obtained 3D data can be further modified and used for various applications in industry [9]. In the agricultural sector, reverse engineering technology helps to create 3D models of agricultural machinery components, where digitization allows to verify the conformity of geometric dimensions and to detect deviations between models [10]. Accurate reconstruction is aided by a modular approach to CAD modelling of assembly, which allows the user to flexibly choose the individual steps of the process [11]. A key problem in reverse engineering is reconstruction of freeform surfaces, especially for geometrically complex parts. By using NURBS curves, readable CAD models with optimal segment curves can be created, which enables more faithful reconstruction of complex parts [12]. Another example is CAD models creation of damaged or obsolete parts, where additive manufacturing facilitates the restoration of functionality of components [13]. To ensure high accuracy of the resulting model, photogrammetry methods are often used, which allow accurate 3D scanning of machine parts and elimination of distortions using laser triangulation [14]. CAD technology also contributes to the efficient extraction of line features from images of industrial components, which ensures high accuracy in contour reconstruction [15]. Process planning for reverse engineering methods is also very important, as a correctly chosen number of scans ensures higher accuracy of the resulting model and eliminates the need for repeated scanning processes [3]. Reverse engineering also finds application in the construction of complex components, such as turbine engine blades, where 3D scanning and inspection on coordinate measuring machines ensure the accuracy of the models [16].

The research results show that reverse engineering is a powerful tool for digitization and reconstruction of complex industrial components, while enabling the extension of device life cycle and optimization of product design thanks to modern measurement technologies and digital twins. Reverse engineering is an indispensable tool in the industrial toolkit. It fosters innovation by allowing engineers to understand and improve upon existing designs. As technologies evolve, the precision and efficiency of reverse engineering will continue to advance, offering even greater benefits to industries. Benefits of reverse engineering technology are manifold. It accelerates product development cycles, reduces research and development costs, and enables manufacturers to analyse materials and components with precision. It also supports customization and improves interoperability by ensuring that new parts fit within existing systems. Despite its advantages, reverse engineering faces several challenges. Moreover, ethical considerations must be addressed when reverse-engineering products. Accuracy

of final reverse-engineered product depends on many factors. Figure 1 describes the reverse engineering process. Most critical point (from the point of view of digital twin accuracy) is accuracy of input data. That is, with what accuracy we can extract data from real components. Common accuracy verification tests [17] are based on acceptance and re-verification tests of measuring devices. Although these tests are standardized, they do not describe the behaviour of measuring devices on real machine components. The main reason is idealized artifacts. Today, many research institutes are engaged in the development and research of new artifacts with complex shapes. One example is the development of HP 300 artifact. [18] Often, reversed products are subsequently manufactured (not just the construction of a CAD model). A suitable technology to produce reversed parts is 3D printing. Evaluating the accuracy of 3D printed parts using SLS technology is described in [19] or [20].

For the reasons mentioned, it is very important to know the behaviour of measuring devices on real components. The essence of this article is to investigate accuracy of optical scanners on high-gloss freeform artifact.

3 Methodology

All measurements were performed on the freeform artifact Pharaoh, developed at Institute of Technical Mathematics, Faculty of Mechanical Engineering, CTU in Prague.

3.1 Freeform artifact Pharaoh

Surface of the artifact is inspired by head of the dummy for testing electroacoustic systems. The surface of the artefact consists of a cut-out of the most structured part of the dummy's head, i.e. the face. Artifact with dimensions 150 x 175 x 90 mm is made from aluminium alloy and manufactured by milling and polishing. 3 reference ruby spheres in the corners of the standard are used to define the coordinate system for tactile CMM´s alignment and path planning. [21]

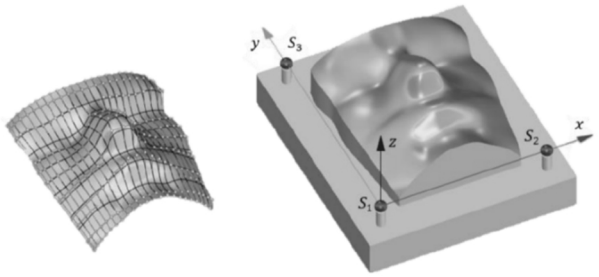

Fig. 2 *Freeform artifact Pharaoh [21]*

3.1.1 Artefact calibration

The artefact was measured in the Primary Metrology Laboratory of Czech Metrology Institute using the Zeiss Xenos Cartesian CMM, which has the status of national standard for 3D geometric dimensions (E0, MPE = 0.3 + L/1000). [21] Tactile scanning was performed in a grid with an average point spacing of 0.5 mm. Tab. 1 summarizes the results of the calibration.

Tab. 1 *Reference tactile measurement results [21]*

Number of scanned points	[/]	45 078
Sample standard deviation	s(D) [μm]	24.81
Minimum deviation	D_{min} [μm]	-57.88
Maximum deviation	D_{max} [μm]	76.83
Surface profile deviation (ISO1101)	SP [μm]	153.7

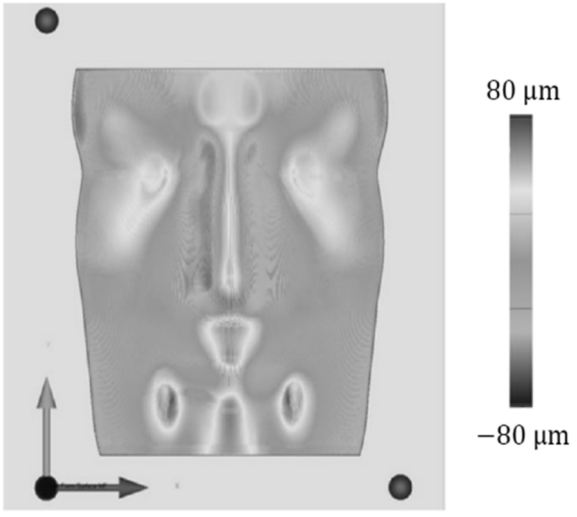

Fig. 3 *Reference measurement – deviations colour map [21]*

Figure 3 shows measured points deviations colour map from nominal values (CAD model) and Table 1 shows the results from reference measurement. Surface was captured in 45 078 discrete points and surface profile deviation is 153.7 micrometers. All measurements will be compared to this reference value. Surface profile deviation was calculated according to ISO 1101 definition [21]:

$$SP = 2 \cdot \max\{|D_{min}|, |D_{max}|\}\ [\mu m] \qquad (1)$$

3.2 Measuring devices

The surface of the Pharaoh artifact was captured using 3 different measuring systems:

- Cartesian CMM LK Altera S with laser scanner Nikon LC15Dx (automated)

- Measuring arm Nikon MCAx S30 with laser scanner Nikon H120 (manual)
- Handheld device Metronor M-Scan 120 with laser scanner Nikon H120 (manual)

Tab. 2 *Specification of measuring devices*

	LK Altera S Nikon LC15Dx	Nikon MCAx S30 Nikon H120	Metronor M-Scan 120 Nikon H120
$P_{Form,\ MPE}$ [μm]	15	50	105

Accuracy specifications of individual measuring systems represented by parameter $P_{Form,\ MPE}$ according to ISO 10360 are presented in Tab. 2. According to the specification, the measuring systems are ranked in the table from the most accurate with the highest level of detail (Altera and LC15Dx) to the least accurate (Metronor and H120). On both manual measuring systems, the measurement is realized with the same Nikon H120 portable scanner. The difference in specification is due to the different scanner carrier (measuring arm and camera system).

Surface scanning of the artifact was performed in 10 repetitions in each case. Stereolithographic mesh was created from measured points and then fitted to the nominal geometry using the best-fit alignment. These steps were done in Polyworks 2024.

3.3 Measurement evaluation

The aim of the analysis is to determine the limit of applicability of individual measuring system in terms of tolerance bandwidth. The limit of applicability is limiting permissible value of measurement capability. The analysis is performed using the two most commonly methodologies in automotive industry: according to VDA (Verband der Automobilindustrie, DE) [22] and AIAG (Automotive Industry Action Group, USA) [23].

3.3.1 Surface profile deviation

For each measurement, surface profile deviation SP according to ISO 1101 and Formula 1 was evaluated. The average value of the surface profile deviation corresponding to the measuring system is evaluated from the partial values according to the Formula 2. [24]

$$\overline{SP} = \frac{1}{n}\sum_{i=1}^{n} SP_i \ [\mu m] \tag{2}$$

3.3.2 Capability based on VDA 5

VDA 5 methodology defines capability ratio Q_{MS} according to the Formula 3. [22]

$$\mathrm{Q_{MS}} = \frac{2 \cdot \mathrm{U_{MS}}}{\mathrm{T}} \ [\%] \tag{3}$$

Where:

T…Tolerance bandwidth;

U_{MS}…Combined measurement uncertainty of measuring system.

$$\mathrm{T} = \mathrm{USL} - \mathrm{LSL}\ [\mu m] \tag{4}$$

$$\mathrm{U_{MS}} = \mathrm{k}.\sqrt{\mathrm{u_{CAL}^2} + \mathrm{u_{EVR}^2} + \mathrm{u_{BI}^2} + \mathrm{u_{LIN}^2} + \mathrm{u_{MS.REST}^2}}\ [\mu m] \tag{5}$$

As can be seen from definition of the parameter, 5 sources of measurement uncertainty are considered. The following sources will be considered in the analysis:

- u_{evr}…Repeatability,
- u_{BI}…Systematic measurement error (bias).

$$\mathrm{u_{EVR}} = \sqrt{\frac{1}{9}\cdot\sum_{\mathrm{i=1}}^{10}(\mathrm{SP}_i - \overline{SP})^2} \ [\mu m] \tag{6}$$

$$\mathrm{u_{BI}} = \frac{\left|\overline{SP} - SP_{ref}\right|}{\sqrt{3}} \ [\mu m] \tag{7}$$

Where:

$\overline{SP}$…Arithmetic mean of the repeat measurement

SP_{ref}…Reference value of the surface profile deviation (determined by calibration as 153.7 μm). [22]

Extension coefficient k for the coverage of 95.4 % according to the Gaussian distribution is set to k=2.

The minimum tolerance bandwidth T_{min} according to VDA 5 is determined using a modified formula (Formula 8). The calculation considers the limit value of the capability ratio Q_{MS} = 15 % recommended by VDA 5.

$$T_{min} = \frac{2 \cdot U_{MS}}{0.15} \cdot 100\ [\mu m] \tag{8}$$

3.3.3 Capability based on MSA 4

The evaluation is performed using the measurement capability index C_{gk} which, unlike the C_g coefficient, considers measurement repeatability and bias. The Bosch methodology is used, which considers a 20 % of tolerance bandwidth. [23]

$$\mathrm{C_{gk}} = \frac{0.1 \cdot T - |\bar{x} - x_m|}{3 \cdot s_g} \ [/] \tag{9}$$

Where:
X_m…Reference value,
$\bar{x}$…Mean value of repeat measurements,
T…Tolerance bandwidth,
s_g…Sample standard deviation of repeat measurements.

A modified equation (Formula 10) is used to evaluate the minimum width of the tolerance field to ensure a capable measurement according to MSA 4. The calculation is based on the limit value of the index C_{gk} = 1.33 (acc. to Bosch methodology). [23]

$$T_{min} = \frac{399 \cdot s_g}{10} + 10 \cdot \left|\overline{SP} - SP_{ref}\right| \ [\mu m] \tag{10}$$

4 Preliminary – evaluation post-processing parameters settings in Polyworks software

Polyworks software offers 4 basic data acquisition settings profiles: Extra fine, Fine, Standard and Coarse. Individual types of settings are different from each other primarily by level of data filtering (filtering according to the maximum angle of inclination – the maximum possible deviation of the sensor from the normal orientation with respect to the measured surface, etc.), smoothing and reducing triangles of polygon mesh. Polyworks allows you to set all these parameters even before the points are extracted from the surface because the subsequent fitting of the polygon mesh can already be automated (increasing the efficiency of measurement and data processing). This process is referred to as Real-time quality meshing. The individual settings profiles differ from each other in the parameters described in Table 3.

Tab. 3 *Analysis of profiles in Polyworks*

Parameter setting (profile)	Distance of neighbouring points [mm]	Maximum edge length of triangle [mm]	Maximum angle of inclination [°]	Smoothing / reducing triangles
Extra fine	0.05	1	75	no / no
Fine	0.15	2	75	yes / yes
Standard	0.25	4	75	yes / yes
Coarse	0.40	4	75	yes / yes

It can be seen from Table 3 that the Fine, Standard and Coarse settings profiles already use source data filtering and optimization of the generated polygon mesh. Due to further intervention in the scanned points by software, it is necessary to specify the parameters that affect the filtering (here reduction of triangles) and smoothing. An overview of the parameters can be seen in Table 4.

Tab. 4 *Description of settings profiles*

Parameter setting (profile)	Smoothing		Reducing	
	Maximum radius curvature (mesh vertices) [mm]	Maximum possible displacement of a point [mm]	Triangle reduction level (how much remains) [%]	Maximum edge length of triangle [mm]
Extra fine	/	/	/	/
Fine	0.30	0.025	80	2
Standard	0.50	0.050	80	2.5
Coarse	0.80	0.050	80	3.5

Measuring arm MCAx and scanner H120 were chosen to test all four scanning setups. The technology was chosen due to the simplest preparation of measurements without programming or positioning of the camera system. Arm and scanner can be considered the most time-efficient method for starting measurement (of those compared in the experiment). A surface scan of the artifact was performed in 10 repetitions for each setup. A polygon mesh was created from the measured points and then aligned to the nominal geometry using the best-fit alignment. Table 5 presents an overview of all obtained results.

Tab. 5 *Achieved surface profile deviation values*

	Surface profile deviation [µm]										
	SP_1	**SP_2**	**SP_3**	**SP_4**	**SP_5**	**SP_6**	**SP_7**	**SP_8**	**SP_9**	**SP_{10}**	**$\overline{SP}$**
Extra fine	310	1002	541	626	260	254	575	587	489	319	496
Fine	468	406	334	179	248	338	473	378	618	305	375
Standard	176	168	217	175	189	141	156	175	200	201	180
Coarse	155	220	203	224	208	182	232	165	246	203	204

As can be seen from Table 5, the Extra fine profile shows a huge value of unrepeatability of results. Data filtering from outliers is therefore very important for surfaces of a glossy freeform character.

Table 6 and Figure 4 further describe how many points were obtained and how unrepeatable the results are. Point clouds obtained at the Extra fine setting are characterized by the highest density, while this setting does not filter the scanned points. Many resource points are also inappropriate due to the need for more space on the computer's hard drive and greater requirements for computing technology. It is interesting to observe a large difference in the number of source data between the Extra fine and Fine profiles. The use of software filtering on source data for reverse engineering can be observed. Conversely, the coarse setting generates point clouds with the lowest density. It is interesting that too much intervention in the input data leads to larger deviations. This fact can be observed on Coarse profile.

Tab. 6 *Effect of profile settings on number of points and accuracy*

Parameter setting (profile)	Number of measurement repetitions [/]	Number of points [/] (scan 1)	Average surface profile deviation [µm]	Bias from reference value [µm]	Standard deviation [µm]
Extra fine	10	6 441 406	496	343	228
Fine	10	59 744	375	221	125
Standard	10	43 164	180	26	23
Coarse	10	27 565	204	50	29

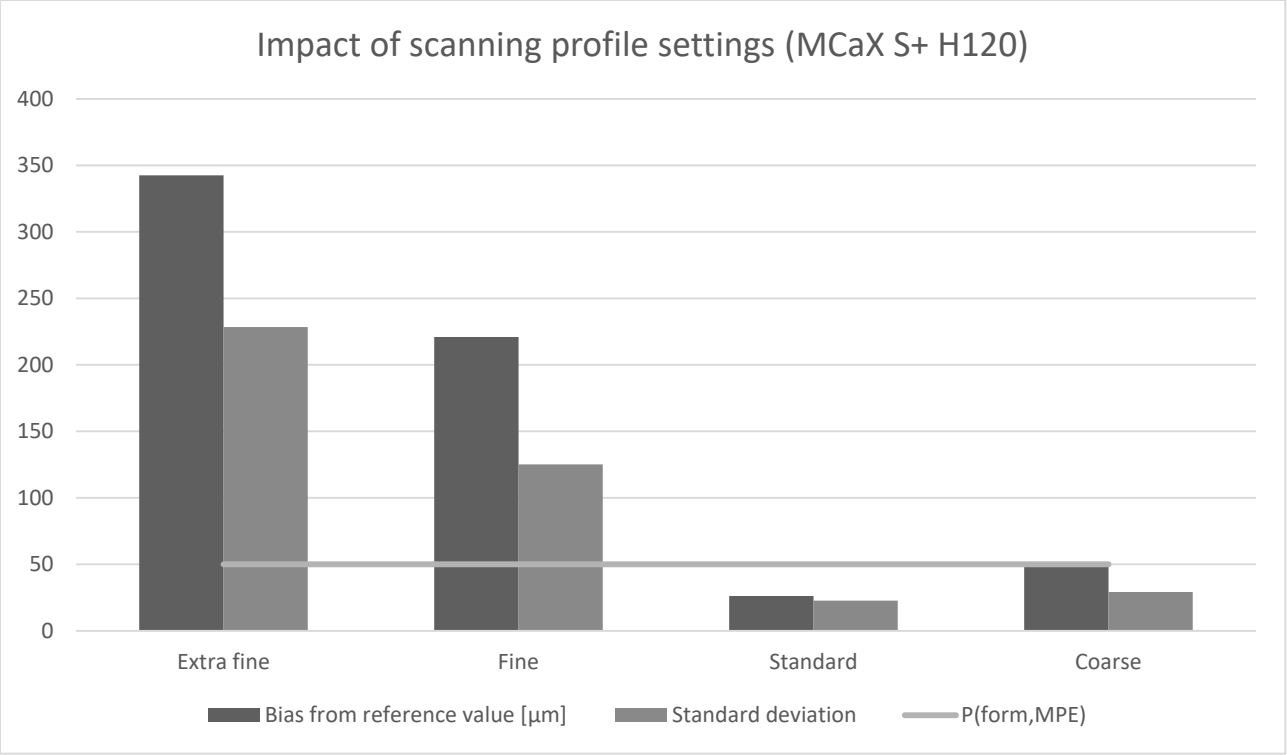

Fig. 4 *Measurement bias for various parameters setting (MCAx and H120)*

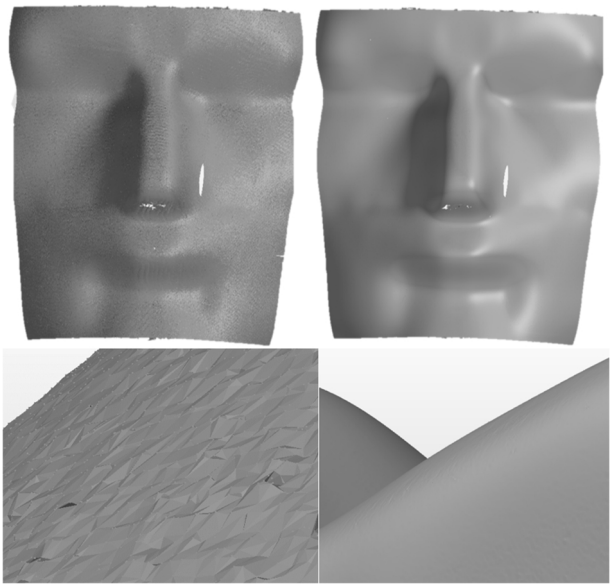

Fig. 5 *Effect of noise reduction in Polyworks (left – Extra fine profile, right – Standard profile)*

Figure 5 demonstrates the qualitative difference in the resulting stereolithography mesh between Extra fine and Standard profile. These two profiles were chosen to achieve the best and worst results. For all subsequent measurements, the Standard profile will be used because it demonstrated lowest bias from reference value and lowest standard deviation on repeated measurements in experiment.

5 Results

5.1 Evaluation of Surface profile deviation for 3 scanning technologies

Surface profile deviation according to ISO 1101 was selected for evaluation. Table 7 and Figure 6 shows achieved values for comparing scanning technologies. To ensure the statistical relevance of the results, 10 scan repetitions were performed for all systems, representing a total of 30 scanned point clouds and analysis.

Tab. 7 *Surface profile deviation results, Bias from reference and Standard deviation for each scanning technology*

	Surface profile deviation [µm]											Bias from reference value [µm]	Standard deviation [µm]
	SP_1	SP_2	SP_3	SP_4	SP_5	SP_6	SP_7	SP_8	SP_9	SP_{10}	$\overline{SP}$		
Altera LC15Dx	157	165	157	158	166	170	160	165	158	165	**162**	8	5
MCAx H120	176	168	217	175	189	141	156	175	200	201	**180**	26	23
M-Scan 120 H120	236	273	281	274	291	321	428	320	329	231	**298**	144	57

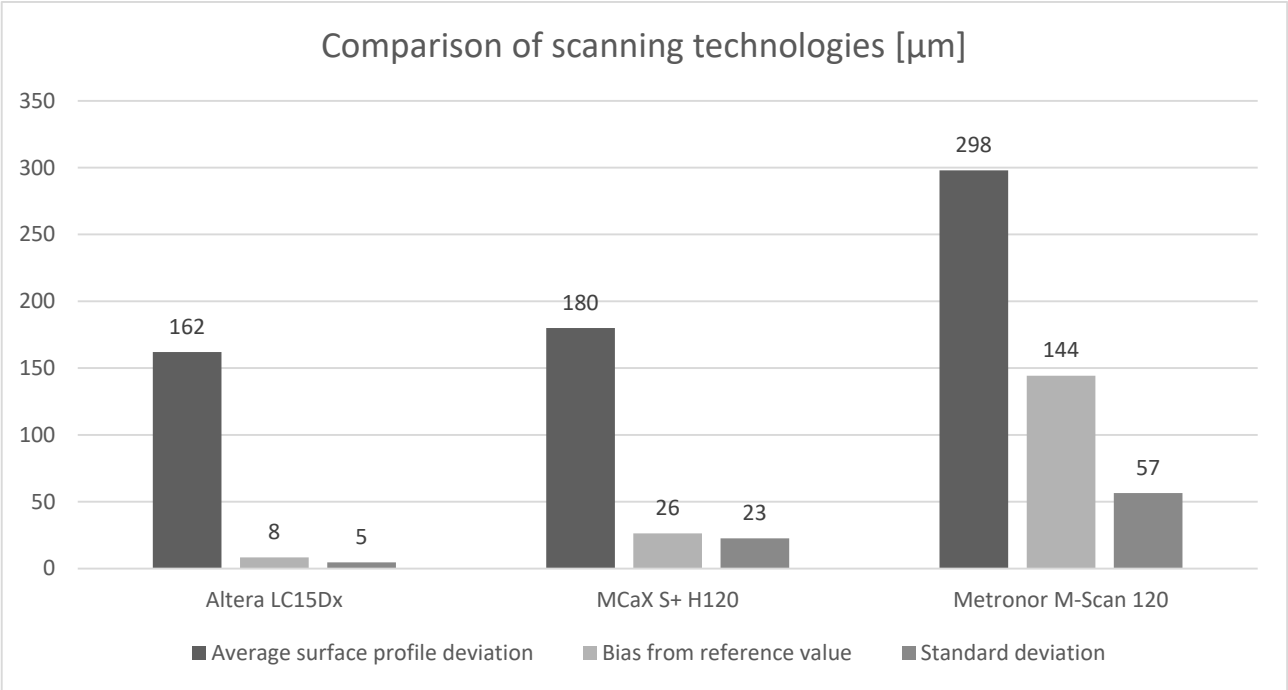

Fig. 6 *Comparison of scanning technologies*

Figure 7 shows 4 color maps. First 3 of them represent the first mesh from repeated measurement by laser scanners and the last one represents the points deviation from tactile measurement. It is important to emphasize that the data evaluation was analyzed in different metrology software. The scanned data was evaluated with Polyworks software and the tactile measurement data was evaluated with Calypso software. This results in shifted colour scales in the color map. Even though there is a difference in the colour scale, we can see the similarity of deviations distribution between the reference measurement and the scanned data.

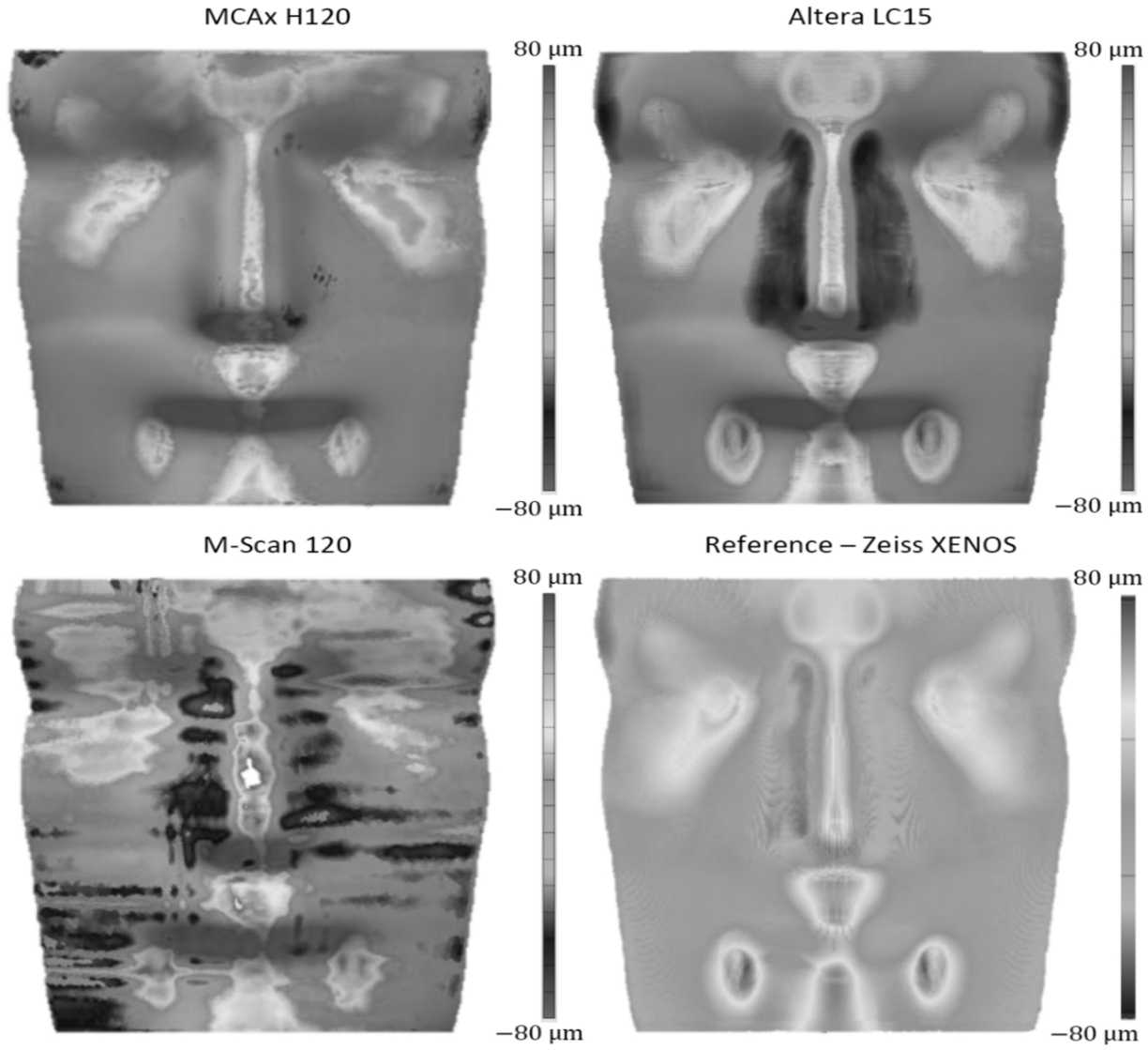

Fig. 7 *Colour map of deviations from the nominal CAD model*

As expected, the scanned data from stationary cartesian CMM (Altera and LC15) are closest to the reference result. Main reason is automated CMM movements and constant scanning speed. The data taken by the measuring arm are more unrepeatable and show more bias from the reference value. And data from handheld scanner with camera system show the greatest deviation from the reference value. A large spread of the laser line can be observed on the color map.

5.2 Determining the minimum possible tolerance zone for each measuring system

Tab. 8 *Measurement results using the VDA methodology*

Measuring system	u_{EVR} [µm]	u_{BI} [µm]	U_{MS} [µm]	T_{min} [mm] VDA 5
Altera and LC15	4.63	4.85	11.61	0.15
MCAx and H120	22.60	15.07	47.05	0.63
M-Scan 120 and H120	56.51	83.54	174.70	2.33

Tab. 9 *Measurement results using the MSA methodology*

Measuring system	T_{min} [mm] MSA 4th edition
Altera and LC15	0.27
MCAx and H120	1.16
M-Scan 120 and H120	3.70

Tab. 10 *Comparison of results from the experiment with measuring systems specifications*

Measuring system	$P_{Form, MPE}$ [mm]	T_{min} [mm] VDA 5	T_{min} [mm] MSA 4th edition
Altera and LC15	0.015	0.15	0.27
MCAx and H120	0.050	0.63	1.16
M-Scan 120 and H120	0.105	2.33	3.70

5.3 Results discussion

Tables 8, 9 and 10 show that the laser scanner Nikon LC15Dx mounted on cartesian CMM LK Altera S is suitable for capable measurement of glossy freeform surfaces manufactured with a tolerance band of approximately 0.15 mm (VDA), respectively 0.3 mm (MSA). Measuring system consisting of measuring arm Nikon MCAx S30 and laser scanner Nikon H120 may be used for capable measurement of parts with a minimum tolerance bandwidth of 0.6 mm (VDA), respectively 1.2 mm (MSA). The Metronor M-Scan 120 with laser scanner Nikon H120 can inspect products with a tolerance band of 2.3 mm (VDA), respectively 3.7 mm (MSA).

Based on the experiment we can say:

- It is difficult to scan reflective (glossy) surfaces for laser scanner technology (consider use of matting sprays for the prevention of reflection),
- High demands of measurement capability in automotive industry based on VDA 5 and MSA 4 methodology leads to high demands on low variability of measuring results,
- Large differences between the specified accuracy values $P_{Form, MPE}$ from acceptance and re-verification tests and minimum tolerance values T_{min} presented for hard to scan glossy surfaces.

6 Conclusion

The article discusses accuracy of 3 measuring systems on glossy freeform artifact. Measurement on such artifact was chosen to determine the deviation in non-ideal conditions (glossy freeform). Conventional acceptance and re-verification tests do not describe the behavior of measuring systems in real conditions. Therefore, the tests in this article monitor the limit behavior of scanners and mainly the optimal settings of post-process parameters in Polyworks software. Comparison of 3 scanning measuring systems is presented and the optimal settings for glossy parts are determined. 3D line triangulation scanners use a method of optical triangulation, in which a laser beam hits an object, and its dispersion is captured by a camera (CCD chip) at a certain angle. Technology is sensitive to the surface properties of the scanned objects, especially their glossiness. There are several reasons. Glossy surfaces have a high reflectivity. Reflectivity causes the light beam to often reflect at unexpected angles. Due to the principle of triangulation, where the exact angle of reflection is essential, changes in the angle of reflection can cause inaccuracies or even loss of detectable signal. In the case of high-gloss materials, light can reflect off the camera view and result in an insufficient or incorrectly captured point. Dispersion occurs on matte surfaces, where light scatters in many directions, allowing the scanner to obtain a clear and stable image of the surface. However, glossy surfaces create a specular reflection, where light hits at one angle and is reflected at the same angle. This kind of reflection can lead to severe camera glare or a complete loss of signal, resulting in data gaps or a distorted surface image. Glossy surfaces can cause a portion of the beam to polarize and scatter. Interference also occurs, where individual parts of the reflected beam overlap, creating noise or inconsistent data. Materials with a glossy surface can have different absorption characteristics, which affects the behavior of the laser beam on the

surface. Some materials can partially absorb the laser light, resulting in weaker signals that are difficult for the camera to detect. These factors make scanning glossy freeform surfaces with line triangulation scanners problematic. One solution is to use sprays or powders that temporarily dull the surface, reducing specular reflection and allowing for more accurate measurements. Of course, the thickness of the applied powder layer must be kept in mind. Alternatively, other modern scanning technologies such as structured light scanners or scanners using phase shift interferometry, which may be less sensitive to the reflective properties of materials, can be targeted. Reflectivity of laser line is investigated, for example, in articles Polarization 3D imaging technology [25], Waviness analysis of glossy surfaces based on deformation of a light source reflection [26].

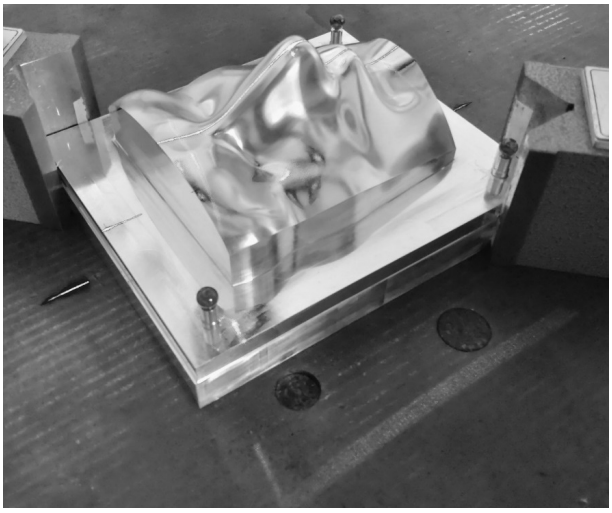

Fig. 8 *Laser beam reflection on the artifact surface*

6.1 Optimal parameters of post-process settings (for glossy surfaces) in Polyworks

Setting the correct parameter plays a key role for correct acquisition of points from a real part. Optimally selected parameters that achieved the best surface profile deviation values in our experiment are:

- Distance of neighbouring points – 0.25 mm
- Maximum edge length of triangle – 4.00 mm
- Maximum angle of inclination – 75°
- Smoothing – Maximum radius curvature – 0.50 mm
- Smoothing – Maximum possible displacement of a point – 0.05 mm
- Reducing – Triangle reduction level (how much remains) – 80%
- Reducing – Maximum edge length of triangle – 2.50 mm

MPE parameters from acceptance and re-verification tests do not correspond to the actual accuracy of measuring systems under complex measurement conditions. The main reason is idealized measurement conditions and artifacts with suitable surface for scanning systems. Despite the fact that the scanning systems had a valid calibration certificate from re-verification test at the time of experiment, scanning of hard-to-scan surfaces shows such values. The aim of the experiment is to determine the limiting behavior of the scanning systems in these non-ideal and real conditions. We recommend always performing an assessment based on MSA or VDA. From these tests the real capabilities of measurement systems can be determined even for reverse engineering applications.

References

[1] KOPTIS MICHAL, JAN URBAN, LIBOR BERANEK, JAN SIMOTA, PETR MIKES. (2017). Application of Reverse Engineering Technology. *Technological forum* 2017 Book of proceedings. Jaromer, Czech Republic. ISBN 978-80-87583-22-7.

[2] WANG, WEGO. (2010). *Reverse Engineering*. CRC Press. ISBN 9781439806319. doi:10.1201/EBK1439806302

[3] GENG, ZHAOHUI, ARMAN SABBAGHI, BOPAYA BIDANDA. (2023). Reconstructing original design: Process planning for reverse engineering. *IISE Transactions*, p. 509-522. ISSN 2472-5854. doi:10.1080/24725854.2022.2040761.

[4] BOUKHAROUBA, TAOUFIK, FAKHER CHAARI, MOUNIR BEN AMAR, KRIMO AZOUAOUI, NOURDINE OUALI, MOHAMED HADDAR, ed. (2019). Computational Methods and Experimental Testing. Mechanical Engineering. Cham: Springer International Publishing. *Lecture Notes in Mechanical Engineering*. ISBN 978-3-030-11826-6.

[5] DEJA, MARIUSZ, MICHAŁ DOBRZYNSKI, MARCIN RYMKIEWICZ. (2019). Application of Reverse Engineering Technology in Part Design for Shipbuilding Industry. *Polish Maritime Research*. 26(2), 126-133. ISSN 2083-7429. doi:10.2478/pomr-2019-0032.

[6] TAM, JULIANA, KAI YU. (2020). Mapping Based Calibration for Integrated Measuring System on Reverse Engineering of Freeform Shape. *Computer-Aided Design and Applications*, 18(4), 644-654. ISSN 16864360. doi:10.14733/cadaps.2021.644-654.

[7] TANG, YONGPENG, YAONAN WANG, HAORAN TAN, WEIXING PENG, HE XIE, XUEBING LIU. (2023). A Digital Twin-

Based Intelligent Robotic Measurement System for Freeform Surface Parts. *IEEE Transactions on Instrumentation and Measurement*, 72, 1-13. ISSN 0018-9456. doi:10.1109/TIM.2023.3261933.

[8] DHIPAKUMAR, R. (2019). Reverse Engineering in Mechanical Components. *International journal of engineering research & technology* (IJERT) confcall. doi:10.17577/IJERTCONV7IS11103.

[9] AMROUNE, SALAH, AHMED BELAADI, MOUSSA MENASERI, NOUREDDINE GEROSKI, BARHM MOHAMAD, KHALISSA SAADA, RIYAD BENYETTOU. (2021). Manufacturing of Rapid Prototypes of Mechanical Parts Using Reverse Engineering and 3D Printing. *Journal of the Serbian Society for Computational Mechanics*. 167-176. ISSN 18206530. doi:10.24874/jsscm.2021.15.01.11.

[10] VERİM, ÖZGÜR, OZAN SEN. (2023). Application of reverse engineering method on agricultural machinery parts. *International Advanced Research and Engineering Journal*, 2023-04-15, 7(1), 35-40. ISSN 2618-575X. doi:10.35860/iarej.1188175.

[11] SHAH, GHAZANFAR ALI, ARNAUD POLETTE, JEAN-PHILIPPE PERNOT, FRANCA GIANNINI, MARINA MONTI. (2022) User-Driven Computer-Assisted Reverse Engineering of Editable CAD Assembly Models. *Journal of Computing and Information Science in Engineering*. ISSN 1530-9827. doi:10.1115/1.4053150.

[12] MARZOOG, R J, A A ALDUROOBI, S S ALZUBAIDY. (2020). Surface segmentation and reconstruction in reverse engineering. *IOP Conference* Series: *Materials Science and Engineering*. 2020-07-01, 881(1). ISSN 1757-8981. doi:10.1088/1757-899X/881/1/012082.

[13] VORKAPIC, MILOS, DANIJELA ZIVOJINOVIC, DRAGAN KRECULJ, TONI IVANOV, MARIJA BALTIC, ALEKSANDAR SIMONOVIC. (2023). Application of additive technology and reverse engineering in the realization of damaged obsolete parts. *FME Transactions*, 51(1), 31-38. ISSN 1451-2092. doi:10.5937/fme2301031V.

[14] MISHCHUK, YEVHEN, ANDRIY SOROCHENKO, YEVHEN BEREZOVSKY. (2023). Use of reverse engineering methods in the process of restoration of machine parts. *Girnichi, budivelni, dorozhni ta meliorativni mashini*. (101), 53-59. ISSN 2709-6149. doi:10.32347/gbdmm.2023.101.0501.

[15] LI, FEI, JACKRIT SUTHAKORN. (2022). Application of CAD Technology in Extracting Line Feature of Industrial Part Image. *Journal of Control Science and Engineering*. ISSN 1687-5257. doi:10.1155/2022/6372168.

[16] KACMARCIK, JOSIP, NERMINA ZAIMOVIC-UZUNOVIC, SAMIR LEMES. Reverse Engineering Using 3D Scanning and FEM Analysis. In: KARABEGOVIC, Isak, ed. (2020). New Technologies, Development and Application III. Cham: Springer International Publishing, p. 285-291. *Lecture Notes in Networks and Systems*. ISBN 978-3-030-46816-3. doi:10.1007/978-3-030-46817-0_32.

[17] HARDING, KEVIN G., SONG ZHANG, B. BOECKMANS, G. PROBST, M. ZHANG, W. DEWULF, J.-P. KRUTH. (2016). *ISO 10360 verification tests applied to CMMs equipped with a laser line scanner*. 986805. doi:10.1117/12.2227061.

[18] SYKORA, J., I. LINKEOVA, P. SKALNIK. (2023). Freeform digital twin approach to develop the HP 300 freeform verification standard. *Measurement*. 218. ISSN 02632241. doi: 10.1016/j.measurement.2023.113227.

[19] MATUS, MIROSLAV, VLADIMIR BECHNY, RICHARD JOCH, MARIO DRBUL, JOZEF HOLUBJAK, ANDREJ CZAN, MARTIN NOVAK, MICHAL SAJGALIK. (2023). Geometric Accuracy of Components Manufactured by SLS Technology Regarding the Orientation of the Model during 3D Printing. *Manufacturing Technology*, 233-240. ISSN 12132489.

[20] TIMKO, PAVOL, JOZEF HOLUBJAK, VLADIMÍR BECHNY, MARTIN NOVAK, ANDREJ CZAN, TATIANA CZANOVA. (2023). Surface Analysis and Digitization of Components Manufactured by SLM and ADAM Additive Technologies. *Manufacturing Technology*, 127-134. ISSN 12132489.

[21] LINKEOVA, IVANA, MARTA HLAVOVA. (2022). CTU freeform standard Pharaoh. Proceedings of the Czech Slovak Conference on Geometry and Graphics. Olomouc: 42nd *Conference* on Geometry and Graphics, 2022. ISBN 978-80-86843-79-7. https://csgg2022.upol.cz/files/gcg_2022-online.pdf.

[22] VERBAND DER AUTOMOBILINDUSTRIE E.V. (VDA). (2021). VDA 5 - *Measurement and inspection Processes*. 3. Prague: CSQ s.r.o.

[23] AIAG STRORE. *Measurement system analysis MSA*. 4. Prague: Czech Society for Quality, 2011, 231 p. ISBN 978-80-02-02323-5.

[24] HUMIENNY, ZBIGNIEW. Can ISO GPS and ASME (2021) Tolerancing Systems Define the Same Functional Requirements. *Applied Sciences*. 11(17). ISSN 2076-3417. doi:10.3390/app11178269.

[25] LI, XUAN, ZHIQIANG LIU, YUDONG CAI, CUNYING PAN, JIAWEI SONG, JINSHOU WANG, XIAOPENG SHAO. (2023). Polarization 3D imaging technology. *Frontiers in Physics*. 2023-5-9, 11. ISSN 2296-424X. doi:10.3389/fphy.2023.1198457.

[26] FILIP, JIRI, RADOMIR VAVRA, FRANK J. MAILE. (2023). Waviness analysis of glossy surfaces based on deformation of a light source reflection. *Journal of Coatings Technology and Research*, 1703-1712. ISSN 1547-0091.